

## RESEARCH ARTICLE

# Enamel histomorphometry, growth patterns and developmental trajectories of the first deciduous molar in an Italian early medieval skeletal series

Stefano Magri<sup>1\*</sup>, Owen Alexander Higgins<sup>1,2</sup>, Federico Lugli<sup>3,4</sup>, Sara Silvestrini<sup>1</sup>, Antonino Vazzana<sup>1</sup>, Luca Bondioli<sup>5</sup>, Alessia Nava<sup>2</sup>, Stefano Benazzi<sup>1</sup>

**1** Department of Cultural Heritage, University of Bologna, Ravenna, Italy, **2** Department of Odontostomatological and Maxillo Facial Sciences, Sapienza University of Rome, Rome, Italy, **3** Institute of Geosciences, Goethe University Frankfurt, Frankfurt, Germany, **4** Department of Chemical and Geological Sciences, University of Modena and Reggio Emilia, Modena, Italy, **5** Department of Cultural Heritage, University of Padua, Padua, Italy

\* [stefano.magri4@unibo.it](mailto:stefano.magri4@unibo.it)



## OPEN ACCESS

**Citation:** Magri S, Higgins OA, Lugli F, Silvestrini S, Vazzana A, Bondioli L, et al. (2024) Enamel histomorphometry, growth patterns and developmental trajectories of the first deciduous molar in an Italian early medieval skeletal series. *PLoS ONE* 19(12): e0304051. <https://doi.org/10.1371/journal.pone.0304051>

**Editor:** Dario Piombino-Mascalci, Vilnius University: Vilniaus Universitetas, LITHUANIA

**Received:** May 6, 2024

**Accepted:** October 4, 2024

**Published:** December 5, 2024

**Copyright:** © 2024 Magri et al. This is an open access article distributed under the terms of the [Creative Commons Attribution License](https://creativecommons.org/licenses/by/4.0/), which permits unrestricted use, distribution, and reproduction in any medium, provided the original author and source are credited.

**Data Availability Statement:** Raw LC-MS data are available on Zenodo: (<https://zenodo.org/records/11059821>). All relevant data are within the manuscript and its [Supporting Information](#) files.

**Funding:** SM is financed by the European Union - NextGenerationEU through the Italian Ministry of University and Research under PNRR - Mission 4, Component 3, Investment 1.3 "Creation of 'enlarged partnerships' between universities, research centres, businesses and funding of basic

## Abstract

Understanding the growth patterns and developmental trajectories of teeth during early life stages provides valuable insights into the ontogeny of individuals, particularly in archaeological populations where such information is scarce. This study focuses on first deciduous molars, specifically investigating crown formation times and daily secretion rates, through histological analysis. A total of 34 teeth from the Early Medieval necropolises of Casalmoro and Guidizzolo (Mantua, Lombardy, northern Italy) were analysed assessing growth parameters and identifying possible differences between sites and between sexes, which are determined through proteomic analysis. Furthermore, a robust linear regression model relating prism length and secretion time was built to estimate growth rates also in teeth in which the finest incremental markings are not visible. The daily secretion rates (DSR) in inner enamel showed a high homogeneity between dental arches, sexes and the two sites. Values fall within the known range reported in the literature for the same tooth class in archaeological populations. However, a difference in DSR was observed when compared with modern sample published values. Crown formation times and age at crown completion differ between dental arches, with maxillary first molars initiating their matrix apposition earlier than mandibular molars as formerly reported. However, no significant differences were highlighted in association with sex. This study expands our understanding of the growth and development of the first deciduous molars in a medieval population, providing valuable insights into growth trajectories specific to the dental arch. These findings highlight the need for extensive investigations using similar methodologies to attain more accurate and comprehensive information about the developmental patterns of first deciduous molars. Additionally, proteomic analysis improves the capability to conduct sex-specific histological assessments of immature individuals, thanks to this method's application in determining their sex.

research projects" (CUP J33C22002850006). FL is supported by the Marie Skłodowska-Curie IF action project AROUSE (grant number 101104566), funded by European Union's Horizon Europe Research and Innovation programme. AN received funding from the European Research Council (ERC) under the European Union's Horizon Europe Research and Innovation Programme (Grant Agreement no. 101077348 – MOTHERS; <https://erc-mothers.eu>) The funders had no role in study design, data collection and analysis, decision to publish, or preparation of the manuscript.

**Competing interests:** I have read the journal's policy and the authors of this manuscript have the following competing interests: three of the authors (LB, FL and AN) are academic editors for Plos One. This does not alter our adherence to PLOS ONE policies on sharing data and materials.

## Introduction

Teeth are an invaluable source of information in bioanthropological studies thanks to their remarkable preservation and resistance to diagenetic alterations [1]. They offer insights into various aspects of human biology and culture [2]. The determination of age at death [3–6], biological growth patterns [7–10], and dietary habits [11–16] are only a few examples of the valuable information that can be extracted from dental remains. Moreover, the analysis of foetal and infant biological life histories through deciduous dentition offers a profound understanding of populational growth trajectories and health status during early life [9, 17, 18].

The presence of incremental growth markers in dental enamel, i.e., daily cross-striations and near-weekly-in humans-striae of Retzius [19, 20], provides insight into the rhythmical development of this tissue. Specifically, cross-striations are the result, among other influences, of a circadian metabolic variation that occurs during the secretion phase of amelogenesis [21–25] which is associated with differential melatonin production throughout the night-day cycle [26–29]. Cross striations are visible under plain transmitted light microscopy as an alternation of dark and bright spots along an enamel prism. On the other hand, striae of Retzius, which appear under plain microscopy as dark bands running from the enamel dentine junction (EDJ) to the outer enamel, are the result of slight variations in matrix secretion due to a still debated biorhythm [20, 30–36]. Moreover, the identification of stress markers, such as Accentuated Lines (ALs, more pronounced striae of Retzius) and the Neonatal Line (NNL, an AL that forms at birth), allows us to identify respectively the occurrence of physiological stressors during dental development and the birth event [9, 37–45]. These latter lines act as permanent records of physiological stress events above a certain threshold—including birth, illnesses, and nutritional deficiencies—which are permanently marked within the enamel's microstructure during its formation [11, 46–49].

By measuring these incremental signatures, we can derive essential parameters such as crown formation times (CFTs; i.e. the time required by ameloblasts—the enamel forming cells—to secrete the whole crown) [50–53], daily secretion rate (DSR; i.e. the daily amount of enamel matrix secreted by an ameloblast) [8, 51, 54–57], and enamel extension rate (EER; i.e. the speed at which ameloblasts are recruited along the EDJ from apex to neck) [58–60]. These parameters ultimately allow us to reconstruct individual dental crown growth trajectories. In particular, first molars in deciduous dentition offer a glimpse into the growth processes during part of foetal development and throughout the first year of childhood [51, 61–64].

Furthermore, the advent of proteomic analysis, particularly the assessment of enamel's amelogenin, has significantly enhanced our ability to determine the sex of individuals through their dental tissues, even in infant remains and in the case of a single tooth [65–68]. Amelogenin is a key protein coded by a gene whose locus is found on the sex chromosomes [69]. The presence of two different isoforms of this protein, namely AMELX (coded by the gene on the X chromosome) and AMELY (coded by the gene on the Y chromosome), allows for determining the individual's sex as male. Conversely, the presence of only AMELX enables the estimation of the individual's sex as female [67]. Until now, osteological sex estimation was limited to adult individuals due to the absence of sexual markers on the bones in juveniles. Hence, this analysis expanded our capability to understand sex distribution and variability in populations.

To date, deciduous dentition has not been investigated as profusely as the permanent one [8, 18, 51, 52, 57, 70–72]. Moreover, among deciduous dentition, many studies have focused on the anterior dental classes [8, 10, 71]. As for the deciduous molars, most studies have examined variability in modern specimens [53, 57], whereas works on archaeological specimens have concerned a few individuals from a specific geographic area [51, 64].

The limited number of studies on archaeological deciduous molars, as well as the observation of a slight discrepancy between the development of pre-industrial and post-industrial

skeletal remains, highlight the need for further investigations into the variability of—especially—deciduous molars. This can be achieved by expanding the populational coverage at both a diachronic and geographic level to create new population-specific reference standards [5, 54, 55, 73, 74].

In this study, we present the histomorphometric analysis of the mesiobuccal cusp of both upper and lower deciduous first molars from inhumed individuals from two Early Medieval Italian necropolises located in the Province of Mantua (Lombardy, northern Italy): Casalmoro and Guidizzolo [75, 76]. The Early Middle Ages in the Italian peninsula followed significant social and demographic changes, with the Lombard conquest of Mantua (602 CE) leading to a process of cultural amalgamation, with shifts in socio-economic structures [77]. Within this context, we aim to explore the variability in CFT and enamel growth trajectories by comparing the two sites. Moreover, we expand our known inter-individual variability and investigate the presence of sexual differences in enamel developmental parameters for deciduous first molars. Finally, the data on daily secretion rates was used to develop a new robust regression formula specifically tailored for pre-industrial populations, as previously proposed for deciduous central incisors [8]. This new linear model can be useful to estimate deciduous first molar odontochronologies in cases where daily incremental structures are not visible.

Overall, this study explores the development of prenatal and postnatal enamel of deciduous first molars, advancing our knowledge on the timing and variability of odontogenesis, and providing valuable insights into biological aspects of two Early Medieval populations from northern Italy.

## Materials and methods

### Archaeological sites and sample

The necropolises of Casalmoro and Guidizzolo, located in the province of Mantua (Lombardy, northern Italy) (Fig 1), were discovered in 1995 and 1996 by the *Soprintendenza Archeologica della Lombardia, Nucleo di Mantova* [75]. The establishment of the two necropolises coincided with the Lombard colonization of northern Italy, which occurred during the 7<sup>th</sup> and 8<sup>th</sup> centuries CE [76].

Both necropolises were characterized by burials organised in parallel rows, with the human remains—mostly fragmentary and in a poor state of preservation—consistently positioned in a west-to-east orientation (Fig 1C and 1D), resembling burial practices of contemporary Lombard necropolises [78, 79]. The few grave goods found in Casalmoro and Guidizzolo primarily consisted of daggers and bone combs, suggesting a potential association with Germanic populations [75]. Based on the general scarcity of grave goods, Ballarini [75] and Menotti [76] suggested these could be locals who partially adopted Lombard burial customs. In total, 60 graves were excavated at Casalmoro, whereas 93 were excavated at Guidizzolo. Among these burials, 19 and 25 (from Casalmoro and Guidizzolo, respectively) were infant individuals. The skeletal collections of Casalmoro and Guidizzolo are kept at the Bones Lab, Department of Cultural Heritage, University of Bologna. All permits were obtained for the described study by the *Soprintendenza Archeologica, Belle Arti e Paesaggio per le Province di Cremona, Mantova e Lodi*, which complied with all relevant regulations.

In this study, a total of 34 first deciduous molars (out of 27 individuals) were selected from infants (of unknown sex before proteomic-based sex determination) from both necropolises. Regarding tooth nomenclature, it was decided to use 'second deciduous molar' instead of 'third deciduous premolar' to ensure comparability with previous studies and to use the terminology most employed in anthropology.

Only the deciduous first molars with the crown completely formed were selected. Moreover, the selection was based on cusp and crown preservation and the absence of carious

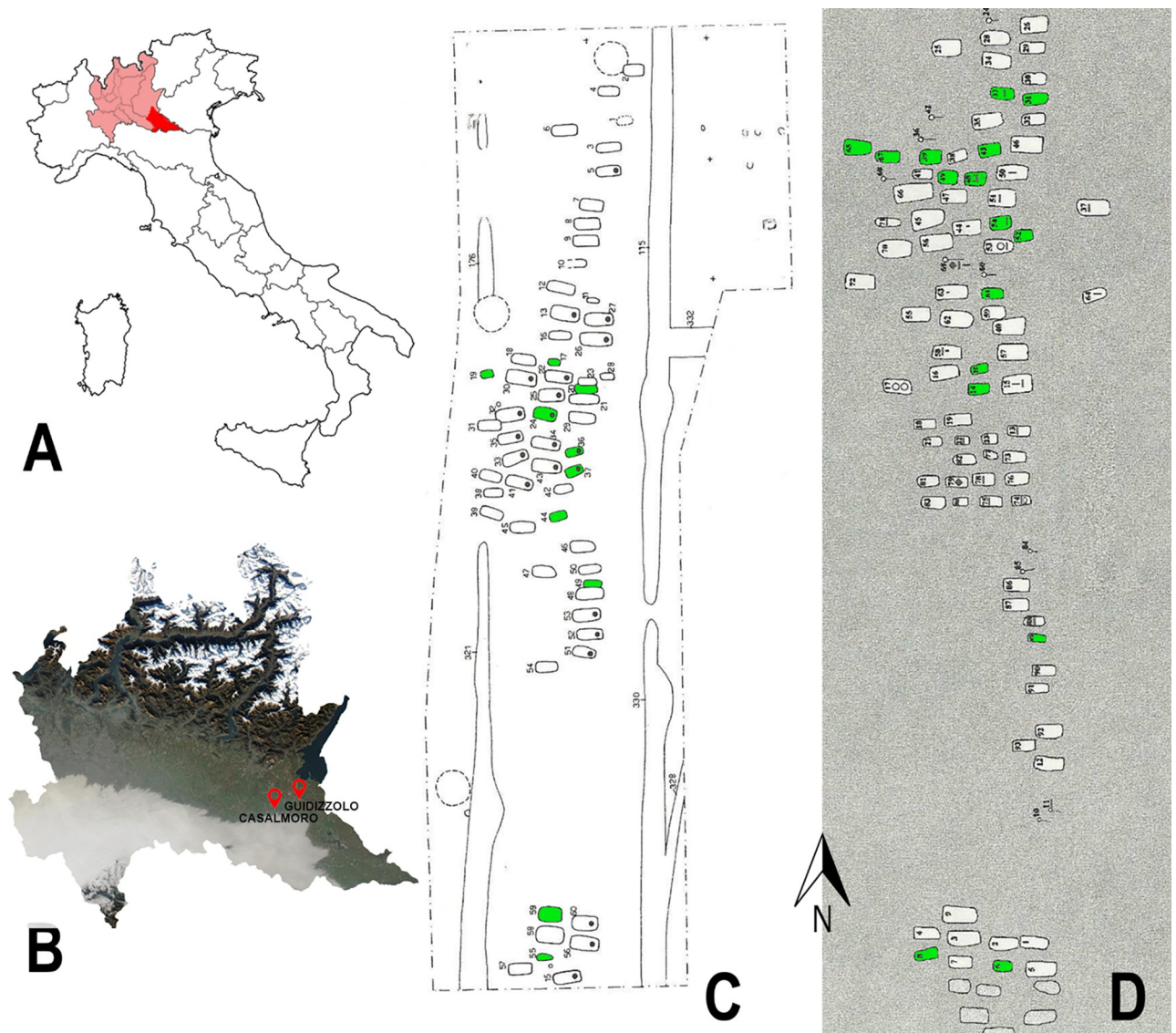


**Fig 1. Geographical location and site plan of the two necropolises.** (A) Position of the Lombardy region (in light red) and of the province of Mantua (in red) within the Italian peninsula; (B) geographic map of Lombardy with the position of the necropolises of Casalmoro and Guidizzolo (map modified from: <https://earthobservatory.nasa.gov/>); (C) excavation plan of the necropolis of Casalmoro; (D) excavation plan of the necropolis of Guidizzolo (in green: the graves investigated in this study).

<https://doi.org/10.1371/journal.pone.0304051.g001>

lesions. Specifically, 13 molars (from 10 individuals) were selected from Casalmoro and 21 molars (from 17 individuals) were selected from Guidizzolo. The wear degree for each tooth was evaluated following Molnar [80].

### Sex determination

Enamel samples (approximately 10 mg) were collected from the distolingual cusp of each tooth before histological processing using a precision drill. Each fragment was cleaned with MilliQ (Milli-Q Millipore) water in an ultrasonic bath and then briefly treated with a 5% HCl solution. To extract the peptides, the enamel samples underwent demineralization using a 5% HCl solution for 1 hour. The resulting supernatant was subjected to purification by  $C_{18}$  in-house stage tips, followed by elution with 50  $\mu$ L of 60% acetonitrile in 0.1% formic acid [67,

[68]. The whole laboratory protocol was performed at the Proteomic facility of the BONES Lab (University of Bologna).

Subsequently, the dehydrated samples were analysed by LC-MS using either the Nano UHPLC Ultimate 3000 coupled to an Exploris™ 480 Hybrid Quadrupole-Orbitrap™ Mass Spectrometer or the Dionex Ultimate 3000 coupled to a HR Q Exactive mass spectrometer (Thermo Scientific), located at *Centro Interdipartimentale Grandi Strumenti* of the University of Modena and Reggio-Emilia, following Lugli et al. [67] and Granja et al. [81]. Ion chromatograms were manually inspected using Xcalibur™ (Thermo Scientific) and sex estimation followed the presence or absence of peaks associated with the two distinct isoforms of amelogenin that are encoded by the two sexual chromosomes: AMELX-(44–52) ( $[M + 2H]^{2+}$  540.2796  $m/z$ ) and AMELY-(58–64) ( $[M + 2H^+]^{2+}$  440.2233  $m/z$ ) [67, 82, 83]. No AMEL-peaks were detected in the blank. Raw LC-MS data are available on Zenodo: <https://zenodo.org/records/11059821>.

### Histological analysis

For histological analysis (following [8]), each tooth was embedded in epoxy resin (EpoThin™ 2, Buehler) and sectioned longitudinally through the mesio-buccal cusps with a microtome (IsoMet™ Low Speed Saw, Buehler) equipped with a 300  $\mu\text{m}$  thick diamond blade. The block containing the dentine horn was gently ground with P2500 sandpaper (CarbiMet™, Buehler) and polished with 1  $\mu\text{m}$  polycrystalline diamond suspension (MetaDi™ Supreme, Buehler) on a dedicated polishing cloth (TriDent, Buehler) to remove the blade's scratches. The block was then attached to a glass slide using additional epoxy resin (EpoThin™ 2, Buehler) and sectioned again to obtain a section of  $\sim 300$   $\mu\text{m}$  of thickness. Each section was ground to reach a thickness of  $\sim 150$   $\mu\text{m}$  using a sequence of progressive grit sandpapers (CarbiMet™, Buehler) and polished with the 1  $\mu\text{m}$  polycrystalline diamond suspension on the polishing cloth. A thickness of  $\sim 150$   $\mu\text{m}$  was required for potential future geochemical analyses [7], whereas a thickness of  $\sim 100$   $\mu\text{m}$  is usually recommended for optimal visualization of the microstructure.

Micrographs of the thin sections were taken at 10x magnification using a high-resolution camera (Axiocam 208 color, Zeiss) mounted on a transmitted light microscope (Axioscope 7, Zeiss). The single micrographs were mounted automatically by the tiles feature in Zeiss ZEN core v3.8 software, creating a composite image of each section.

Chronologies of crown formation were assessed following the method described in Guatelli-Steinberg et al. [59]. Where the tooth was unworn, the first prism segment measuring 200  $\mu\text{m}$  was drawn from the dentine horn, otherwise from one of the more cuspal prisms available. The stria of Retzius at the end of this first segment was traced down to the EDJ, from which a second 200  $\mu\text{m}$  segment was traced. The procedure was repeated until the neck of the crown (Fig 2). In order to assess the time of the stress events, the chronology of Accentuated Lines was similarly assessed.

For each prism segment, the length of multiple ( $n \geq 6$ ) consecutive cross striations was measured and divided by the corresponding number of cross striations to assess the local mean daily secretion rate (DSR). To estimate the number of days represented by each prism segment, its length was divided by the local mean DSR. The number of days represented by each prism segment was cumulatively summed to obtain the overall crown formation time (CFT). Moreover, by using the Neonatal Line (NNL) as a chronological marker, we distinguished between prenatal and postnatal crown formation, identifying crown initiation (Ci) and crown completion (Cc) times. To estimate average CFTs, teeth lacking the cervical portion ( $n = 2$ ) were excluded, as they provide partial information. Similarly, also teeth which present a worn dentine horn ( $n = 22$ ) were omitted in the CFT and Ci estimation.

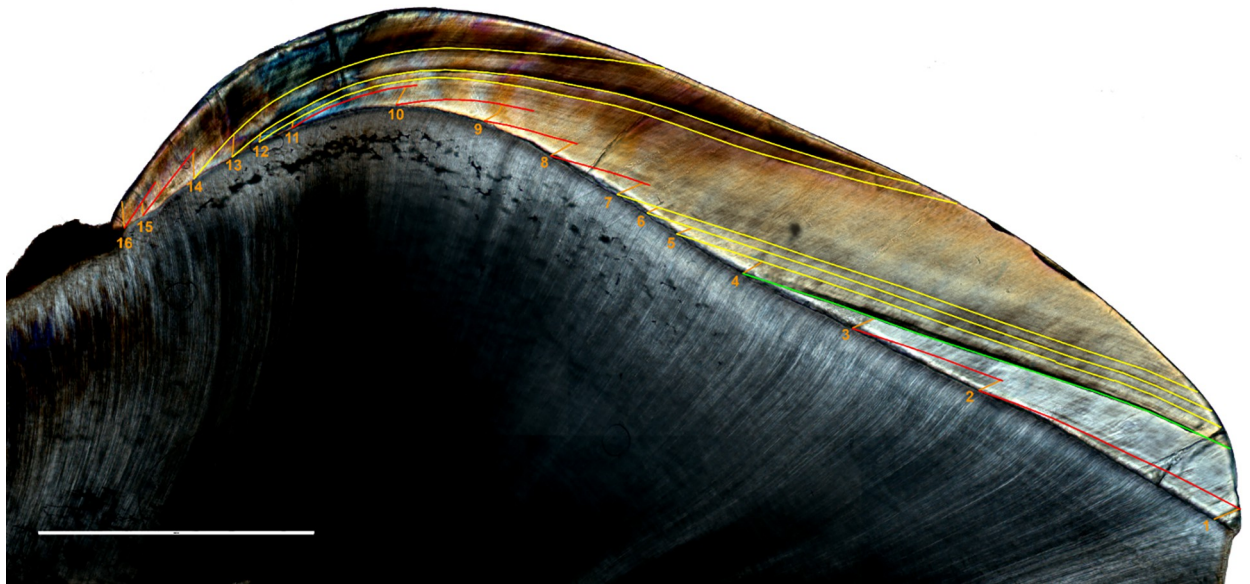


**Fig 2. Thin section of Guid T.61 LR buccal side.** The Neonatal Line (birth marker) is highlighted in green; Retzius Striae are displayed in red; Accentuated Lines (physiological stressor markers) are shown in yellow; enamel prisms are traced in orange. Scale bar = 1000  $\mu\text{m}$ .

<https://doi.org/10.1371/journal.pone.0304051.g002>

Local enamel extension rates were assessed by dividing the length of the EDJ by the estimated number of days.

All lines were traced, and measured with ImageJ (v1.54, National Institute of Health, USA) software [84].

Distances were plotted against cross-striation counts to derive the regression formula for the deciduous first molars. In order to compensate for the presence of possible outliers, a robust regression method was adopted [8], with the constraint of the intercept equal to zero (no prism length equal to no days of enamel matrix production) [85–87].

To observe the relationship between EER and days of formation, a Generalized Additive Model (GAM) [86] was adopted. The model was created as a thin-plate spline interpolation on the dependent variable with a number of degrees of freedom which minimizes the error and the residual deviance.

Five teeth were selected to observe the DSRs ( $n = \sim 400$ ) throughout the entire buccal crown area and were intentionally selected to provide comprehensive representation across both dental arches and sexes following Nava et al. [8] and Peripoli et al. [10]. The topographical maps of the variation in enamel secretion rates were obtained employing a GAM surface interpolation [86]. Indeed, the maps were created by interpolating DSR values across the enamel area, defined by the local coordinates of the sampling points, and digitized through the software tpsDig v.2.05 software [88].

All statistical analyses were carried out using the program for statistical computing R (v.4.3.2) [89] with mgcv [90], robustbase [87], and lava [91] packages. The distribution of values for the various crown parameters was assessed using a Shapiro-Wilk normality test. If the distribution was found to be normal ( $p\text{-value} > 0.05$ ), group variances were compared using an F-test before applying a parametrical test to evaluate the differences. Conversely, if the values did not follow a normal distribution ( $p\text{-value} < 0.05$ ), a non-parametric test was employed to assess the differences.

## Results

Proteomic analysis estimated a total of 8 females and 19 males within the sample. Among the individuals from Casalmoro, 3 were identified as female and 7 as male (S1 Fig), whereas in the sample from Guidizzolo, 5 females and 12 males were identified (S2 Fig). A comprehensive overview of the enamel developmental parameters, wear stage of the mesio-buccal cusp, and estimated sex for each individual is presented in Table 1.

**Table 1. Crown formation times parameters in days, sex, number of accentuated lines and sex of each specimen.** CFT = Crown Formation Time; CI = Crown Initiation; CC = Crown completion; DSR = Daily Secretion Rate; LL = lower left; LR = lower right; UL = upper left; UR = upper right.

ID	Dental Arch	Sex	Wear stage ( <i>Molnar, 1971</i> )	CFT (days)	CI (days before birth)	CC (days)	DSR ( $\mu\text{m}/\text{day}$ )	Accentuated Lines (n)
<sup>a</sup> CA T.17 LL	Lower	M	1	418	199	219	3.05	3
CA T.17 UR	Upper		1	367	174	193	3.18	1
<sup>a</sup> CA T.19 UL	Upper	M	1	353	171	182	3.16	1
CA T.19 LL	Lower		1	401	175	226	3.25	2
CA T.20 UL	Upper	M	3	386	176	210	3.18	1
CA T.24 LR	Lower	M	4	404	149	255	3.10	2
<sup>a</sup> CA T.36 UL	Upper	M	1	358	165	193	3.23	1
CA T.37 UR	Upper	M	2	369	198	171	3.24	0
CA T.44 UL	Upper	M	3	374	180	194	3.23	0
<sup>a</sup> CA T.55 LL	Lower	F	1	401	175	226	3.10	0
CA T.59a LR	Lower	F	2	390	182	208	3.19	1
CA T.59a UL	Upper		3	369	181	188	3.27	0
<sup>a</sup> CA T.59b UL	Upper	F	3	343	166	177	3.17	0
GUID T.6 LR	Lower	F	1	418	185	233	3.15	0
<sup>a</sup> GUID T.8 LR	Lower	M	4	392	135	257	3.12	1
<sup>a</sup> GUID T.14 LR	Lower	M	2	418	175	243	3.08	0
GUID T.20 UR	Upper	M	2	356	181	175	3.21	0
<sup>a</sup> GUID T.31 LR	Lower	F	3	389	165	224	3.11	4
<sup>b</sup> GUID T.33 UR	Upper	F	3	307	195	112	3.19	0
<sup>a</sup> GUID T.39 LR	Lower	M	1	410	179	231	3.24	1
<sup>a</sup> GUID T.43 LR	Lower	M	2	383	150	233	3.21	0
GUID T.43 UR	Upper		3	359	160	199	3.18	0
GUID T.48 LR	Lower	F	2	388	169	219	3.24	0
<sup>a</sup> GUID T.49 LR	Lower	M	2	411	187	224	3.18	3
<sup>a</sup> GUID T.49 UL	Upper		3	357	201	156	3.11	0
GUID T.49b LL	Lower	M	2	408	178	230	3.14	3
GUID T.52 LL	Lower	M	2	378	185	193	3.13	1
<sup>b</sup> GUID T.54 UL	Upper	M	2	n.a.	185	n.a.	3.23	0
GUID T.61 LR	Lower	F	5	398	88	310	3.07	6
GUID T.65 LR	Lower	M	2	383	172	211	3.17	1
GUID T.65 UR	Upper		3	344	187	157	3.15	2
GUID T.67 LL	Lower	M	3	383	164	219	3.19	0
GUID T.67 UL	Upper		3	325	172	153	3.18	0
GUID T.89 UL	Upper	M	3	350	195	155	3.14	4
MEAN				386 (sd = 27) <sup>c</sup>	172 (sd = 19) <sup>c</sup>	208 (sd = 34) <sup>c</sup>	3.17 (sd = 0.26)	

<sup>a</sup> Teeth used for CFT and CI.

<sup>b</sup> Teeth excluded for CC.

<sup>c</sup> Values are calculated based on teeth with an unworn dentine horn or/and an unbroken cervical portion of the crown.

<https://doi.org/10.1371/journal.pone.0304051.t001>

**Table 2. Daily secretion rate values in the inner enamel.** Minimum, maximum, and mean DSR values ( $\mu\text{mday}^{-1}$ ) within 200  $\mu\text{m}$  from the EDJ.

	n	Mean	sd	Min	Max
total	1855	3.17	0.26	2.32	4.33
prenatal	1002	3.20	0.26	2.48	4.33
postnatal	853	3.12	0.25	2.32	4.03

<https://doi.org/10.1371/journal.pone.0304051.t002>

The overall mean inner enamel (within 200  $\mu\text{m}$ ) daily secretion rate—estimated at  $3.17 \mu\text{mday}^{-1}$  ( $n = 1855$ ,  $sd = 0.26$ )—and the minimum and maximum values recorded are reported in Table 2. The prenatal portions of the crowns' buccal aspect exhibit a mean inner enamel DSR of  $3.20 \mu\text{mday}^{-1}$ , whereas the postnatal portions of the same aspect have a mean inner enamel DSR estimated at  $3.12 \mu\text{mday}^{-1}$  (Table 2).

Among Casalmoro's specimens, the mean DSR within inner enamel was estimated at  $3.18 \mu\text{mday}^{-1}$  ( $sd = 0.27$ ,  $n = 706$ ), whereas it was estimated at  $3.16 \mu\text{mday}^{-1}$  ( $sd = 0.25$ ,  $n = 1093$ ) for Guidizzolo (Mann-Whitney U test  $W = 403736$ ,  $p\text{-value} > 0.05$ ). A significant difference arises when comparing prenatal and postnatal portions across both sites (Mann-Whitney U test  $W = 502743$ ,  $p\text{-value} < 0.05$ ). However, the relatively small effect size (Cohen's  $d$  test,  $d = 0.32$ ) suggests that the observed difference may not be practically meaningful. The similarities between the two sites are also evident in the topographic maps of DSR variation across the buccal aspects of five selected specimens (Fig 3). The maps, as expected, exhibited the lowest values in the inner enamel, with DSR values increasing towards the enamel surface, showing an overall similar pattern in all samples.

Overall mean CFT was estimated at 386 days ( $sd = 27$ ,  $n = 12$ ). A difference of ca. 50 days was observed when comparing dental arches (independent t-test for two samples with equal variances  $F = 0.26$ ;  $t = -6.75$ ,  $df = 10$ ,  $p\text{-value} < 0.05$ ). The mean CFT for upper first molars was estimated at 353 days ( $sd = 7$ ,  $n = 5$ ), whereas the mean CFT for lower first molars was estimated at 403 days ( $sd = 14$ ,  $n = 7$ ). No significant differences were observed between sexes (independent t-test for two samples with equal variances  $F = 1.25$ ;  $t = 0.61$ ,  $df = 10$ ,  $p\text{-value} > 0.05$ ) (Fig 4), nor between the sites (t-test for two independent samples with equal variances  $F = 0.41$ ;  $t = 0.40$ ,  $df = 10$ ,  $p\text{-value} > 0.05$ ).

Mean  $C_i$  across the whole sample was estimated at 172 days before birth ( $sd = 19$ ,  $n = 12$ ). Considering the different dental arches, mean  $C_i$  was estimated at 176 days ( $sd = 17$ ,  $n = 5$ ) for upper deciduous molars, and 171 days ( $sd = 20$ ,  $n = 7$ ) for lower deciduous molars. This difference is not statistically significant (Mann-Whitney U test  $W = 17$ ,  $p\text{-value} > 0.05$ ), and no significant dissimilarities are observed between males and females (independent t-test for two samples with equal variances  $F = 14.29$ ,  $t = 0.78$ ,  $df = 4.96$ ,  $p\text{-value} > 0.05$ ) (Fig 5).

The mean age at  $C_c$  across the whole sample was estimated at 208 days ( $sd = 34$ ,  $n = 32$ ) after birth. Comparing dental arches, lower first molar crowns are completed later than upper molars, with a mean  $C_c$  of 231 days ( $sd = 25$ ,  $n = 18$ ) after birth, compared to 178 days ( $sd = 18$ ,  $n = 14$ ) after birth for the upper molars (Mann-Whitney U test  $W = 247$ ,  $p\text{-value} < 0.05$ ) (Fig 6). When sex is taken into consideration, mean  $C_c$  is estimated at 203 days ( $sd = 32$ ,  $n = 24$ ) and 223 days ( $sd = 40$ ,  $n = 8$ ) after birth in males and females, respectively, with no statistically significant difference (t-test for two independent samples with equal variances  $F = 0.62$ ,  $t = -1.43$ ,  $df = 30$ ,  $p\text{-value} > 0.05$ ) (Fig 6).

Enamel extension rate (EER) trends along the crowns' longitudinal growth are illustrated in Fig 7. Irrespective of the dental arch, the trends along the enamel-dentine junction (EDJ) remain relatively consistent. As expected, ameloblasts' recruitment is rapid in the cuspal portion and progressively decreases in speed until birth. In postnatal enamel, the speed remains

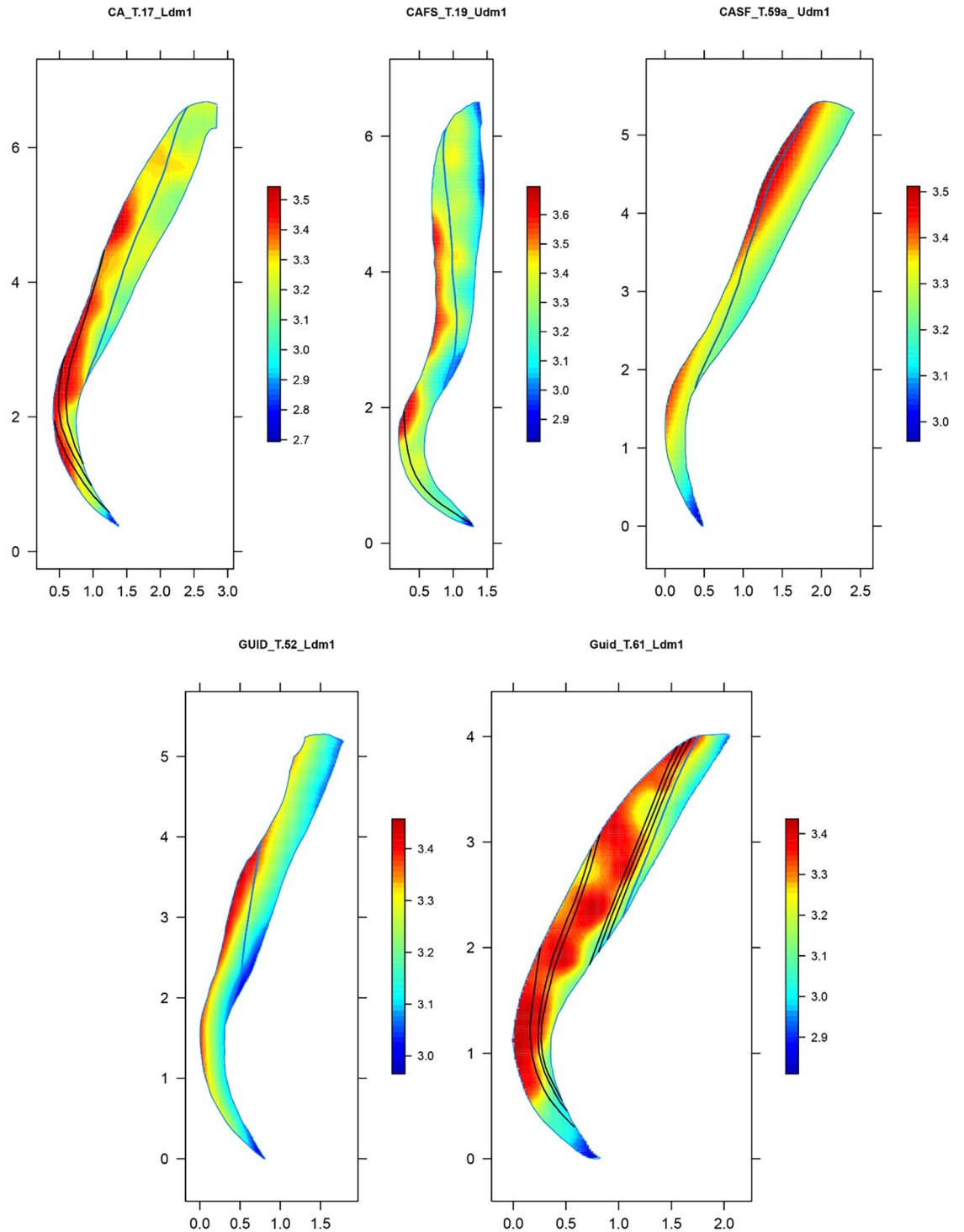


**Fig 3. Maps of the topographic distribution of daily secretion rates in the whole mesio-buccal enamel of five individuals.** X and Y axes report the topographic coordinates; colour bar = DSR value.

<https://doi.org/10.1371/journal.pone.0304051.g003>

relatively constant, with slight changes coinciding with the presence of Accentuated Lines (ALs) (S4 Fig). Finally, as expected, the speed of ameloblast recruitment decreases to its lowest in proximity to the cervical area.

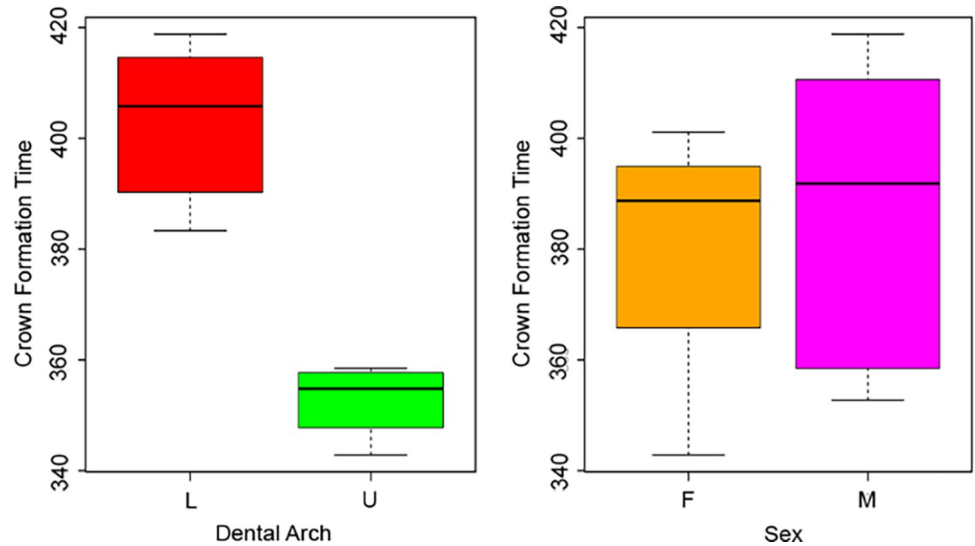


**Fig 4. Boxplots of the variation of crown formation time.** Boxplots show the variation of CFT depending on arches and sexes.

<https://doi.org/10.1371/journal.pone.0304051.g004>

The robust linear regression model (Fig 8) formulated specifically for first deciduous molars, following Nava et al. [8] work on deciduous incisors, can be represented as  $Y = 0.316 X$  ( $Y =$  prism lengths;  $X =$  days) with an adjusted  $R^2$  equal to 0.998 to be considered as indicative only because the intercept was forced to be zero [8].

## Discussion

Acquiring detailed information on the timing of dental formation is crucial for estimating growth rates and ontogenetic trajectories during the early stages of life, as proxied by dental growth. This is particularly critical when dealing with archaeological populations, for which such data are more challenging to obtain.

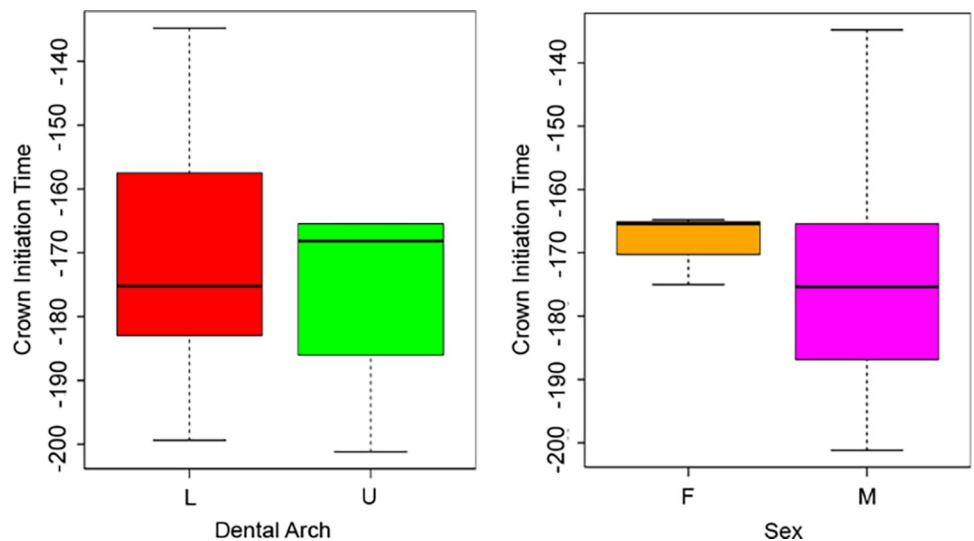


**Fig 5. Boxplots of the variation of crown initiation.** Boxplots show the variation of Ci depending on arches and sexes.

<https://doi.org/10.1371/journal.pone.0304051.g005>

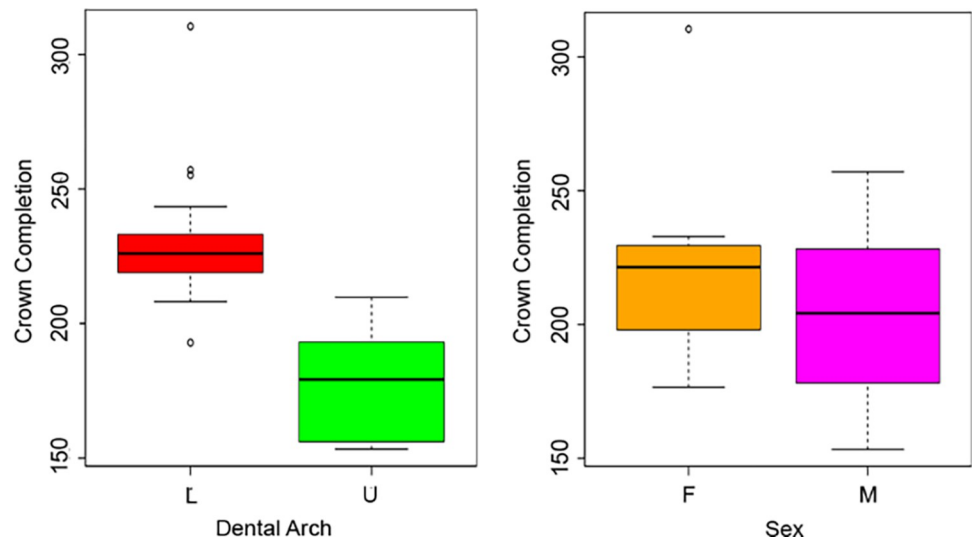


**Fig 6. Boxplots of the variation of crown completion.** Boxplots show the variation of Cc depending on arches and sexes.

<https://doi.org/10.1371/journal.pone.0304051.g006>

In this study, which entails a comparative analysis of two necropolises from the same period (Early Middle Ages) and geographic area (ca 15 km apart), we observe a significant homogeneity in inner enamel DSRs (Figs 8 and 9).

The values observed in this study indicate a lower inner enamel daily secretion rate in the deciduous molars of this medieval cohort compared to reported modern populations [57]. This finding is in opposition to the results of Aris [55] regarding permanent molars, as well as those of Aris et al. [54] and Nava et al. [8] for deciduous anterior teeth. These works reported a decrease in enamel DSRs over time, suggesting a trend towards a slower developmental pace in human recent evolution. Anyhow, it is worth noting that McFarlane et al. [57] did not differentiate between first and second deciduous molars, which could have potentially influenced the DSR's modern comparative values. Overall, the trend of daily secretion rates throughout the entire buccal aspect is consistent with previous observations on deciduous molars [51, 64, 70]. The lowest values are consistently observed in the inner enamel along the EDJ, with a slight further decrease around the cuspal region, the Neonatal Line and the cervical portion (Fig 3). When comparing the daily secretion maps with those presented in earlier studies [8, 10] the distribution trend remains similar to that recorded in anterior teeth, albeit with generally lower DSRs compared to incisors and canines. However, an exception is noted in the case of Guid T.61 LR, which exhibits a more irregular pattern, potentially linked to the presence of a significant number of ALs ( $n = 6$ ) in postnatal enamel, as ALs represent stressful events in an individual's life that affect ameloblast activity [21] (Fig 2).

The linear regression models of the upper and lower arches (Fig 8. S3 Fig) confirm a consistency in DSRs within inner enamel and appear similar to previously regressed models [8, 53]. The slope of this new model is comparable to the one published by Birch and Dean [53], but the intercept is forced to 0, reflecting that no enamel is secreted at day zero.

The mean time of crown formation for the lower first deciduous molars, estimated at 403 days, aligns closely with the findings of Mahoney [51], who reported an average CFT of 388 days on a sample of 12 first deciduous molars. However, our result differs notably from the average CFT of 326 reported by Birch and Dean [53]. This discrepancy with the results of Birch and Dean [53] may however be attributed to the broad variability observed in human

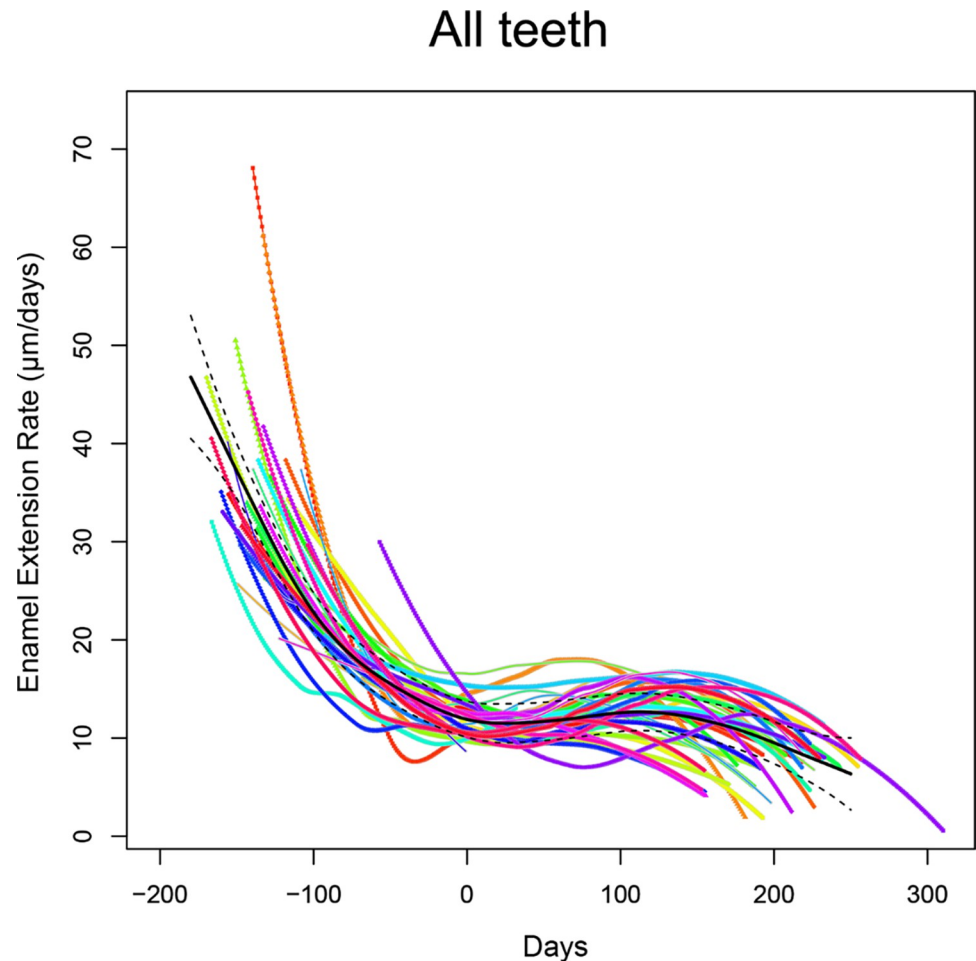


**Fig 7. Enamel extension rate trend across the crown chronologies.** EER trend is represented by a generalized additive model, built as a thin-plate spline interpolation. The black line shows the mean trend of EER in the entire sample.

<https://doi.org/10.1371/journal.pone.0304051.g007>

populations. In contrast, the estimated mean CFT for upper molars, calculated at 353 days, shows a deviation from the findings of Mahoney [64], who reported a mean CFT of 398 days. Nonetheless, our results are within the range of variability noted in the latter work, which reported CFTs ranging from 336 to 510 days for upper deciduous first molars. The higher CFT identified in lower molars compared to upper molars (as illustrated in Fig 3) can be attributed to the greater length of the EDJ, as EERs are comparable (Fig 7). Additionally, the divergence in CFTs observed between the two sites (Fig 10B) may be a sample size bias.

Differences were observed between dental arches for Cc but not for Ci. As far as time at Ci is concerned, our results indicate that deciduous first molars started their enamel secretion at a mean of 172 days (sd = 19) before birth, which corresponds to approximately 3.5 months after fertilization (Fig 5). Whereas the upper first molars reached Cc around one month before the lower molars (Fig 6). Ci estimates for both sites are earlier than what was previously reported by Mahoney [51, 64], who assessed a mean Ci of 113 days before birth, and Birch and Dean [53] who reported a Ci of 140 days before birth. However, our results fall within the range of variability reported by Lunt and Law [92] and Hillson [93], which is comprised between 3.5 and 4.3 months after fertilization (S1 Table). Cc estimates also differ from Mahoney [51, 64]

## Upper and Lower dm1

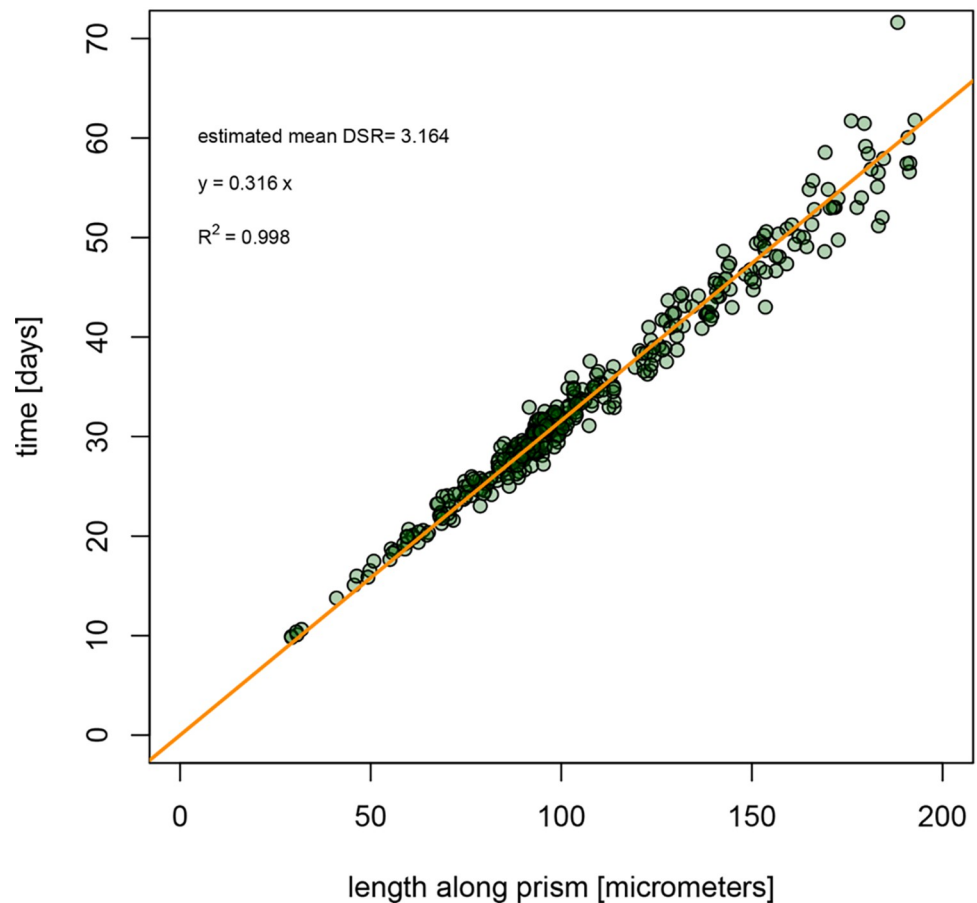


**Fig 8. Linear model to estimate the crown formation time from prism lengths on first deciduous molars.** The regression formula is  $Y = 0.316 X$  ( $Y$  = prismatic lengths;  $Y$  = days) with an adjusted  $R^2$  equal to 0.998.

<https://doi.org/10.1371/journal.pone.0304051.g008>

(275 days), falling however within the range of variability reported in Lunt and Law's review [94] (165–182 days) and being close to the findings of Birch and Dean [53], that found a Cc of 180 days in their sample (S1 Table). The most evident outlier observed in the boxplots (Fig 6) is represented by Guid T.61 LR, which reaches Cc at 310 days after birth. As the CFT of this specimen aligns with those of the other specimens in the sample, this result is likely associated with a delayed Ci (estimated at 88 days pre-birth; Table 1), or/and potentially with a pre-term birth, leading to an extended period of post-birth development. This is also indicated by the more apical position of the NNL compared to the other teeth (Fig 3). In addition, the presence of a high number of ALs may be associated with a change in DSRs during stressful periods [50, 70, 95], this, in turn, can influence the odontochronology.

Upon examining the enamel growth parameters in relation to sexes, no differences were detected. This suggests that the developmental pace in deciduous teeth is not influenced by sex. These findings contrast with some previous studies, which observe a slight advancement in male dental development [96, 97]. However, it is worth noting that differences in skeletal development between sexes are commonly known [98]. It is important to consider that in our samples the sex ratio is skewed toward males, comprising approximately 70% of the

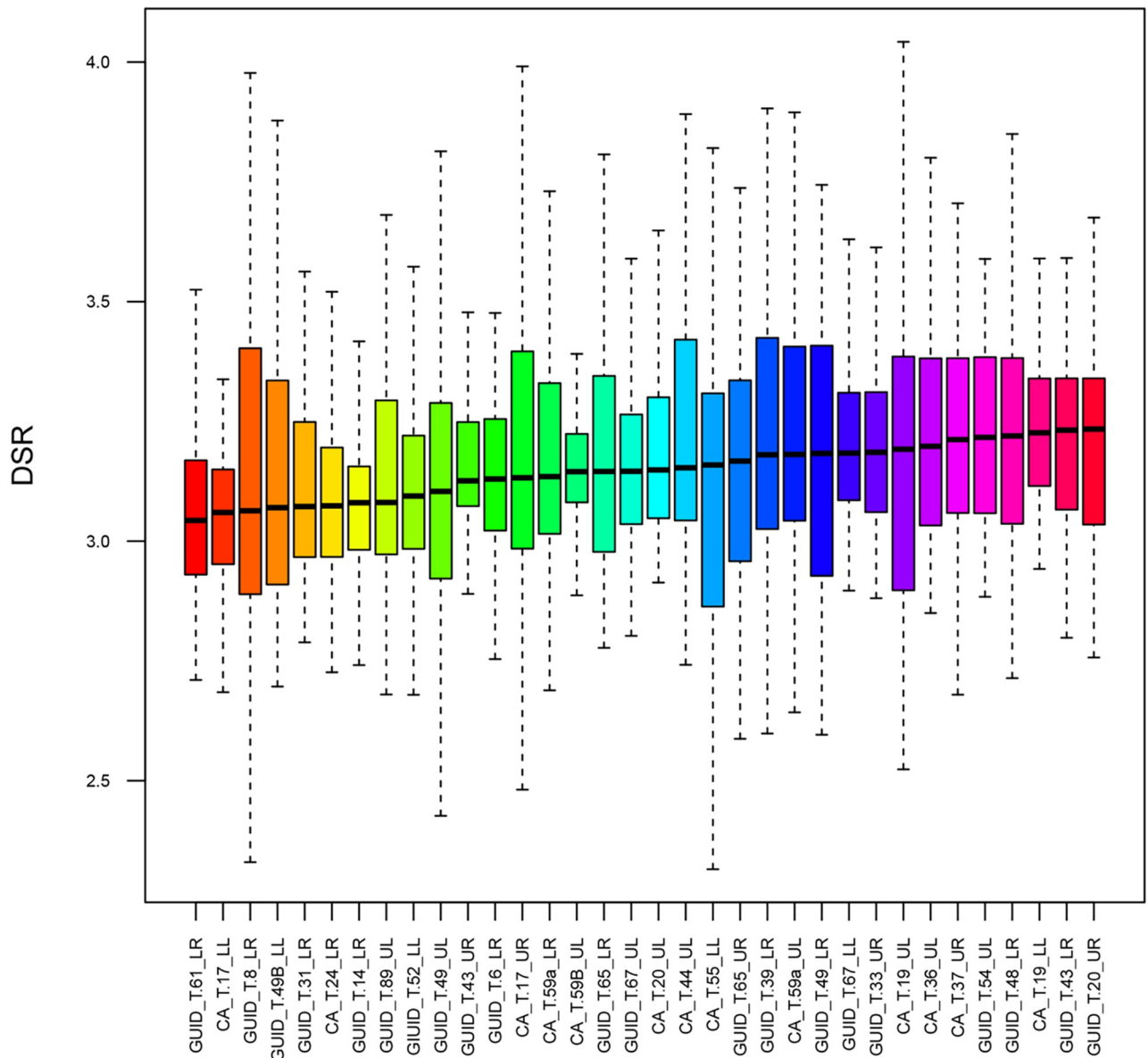


**Fig 9. Boxplots of inner enamel DSR values for each tooth.** Boxplots show the DSR distribution in the entire sample, ordered by increasing median values. Each colour represents one individual.

<https://doi.org/10.1371/journal.pone.0304051.g009>

individuals. This imbalance in the sample composition may have implications for the interpretation of our findings and suggests further investigation into histological aspects of deciduous teeth considering sex.

Finally, the lack of significant differences in all evaluated parameters between the two necropolises (Fig 10) is consistent with observations made by Ballarini [75] and Menotti [76] regarding the similarity—and potential interrelationship—between these two groups, for which certain details of the burial customs set them apart from other allochthonous groups within the same geographic area. This observation warrants further and broader investigations that could provide valuable insight into population dynamics in Northern Italy plains during the Early Medieval period.

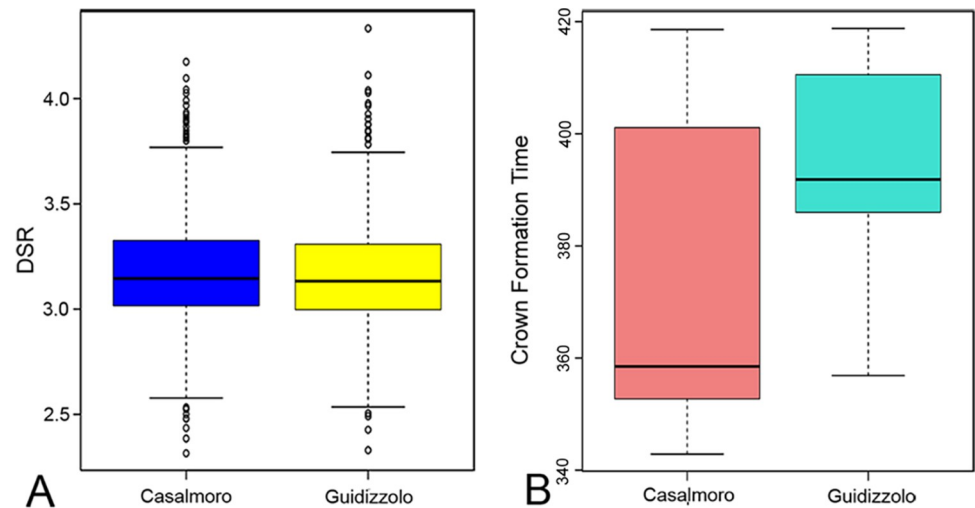


**Fig 10. Boxplots of DSR and CFT variation between two sites.** Boxplots compare (A) daily secretion rates and (B) Crown Formation Time from the two necropolises. A marginal yet non-significant distinction was identified only in Crown Formation Time.

<https://doi.org/10.1371/journal.pone.0304051.g010>

## Conclusions

This study contributes to the existing knowledge on developmental patterns of first deciduous molars by collecting data with high temporal accuracy, enabling the assessment of both prenatal and postnatal enamel formation within two archaeological populations from Early Medieval northern Italy. The development of a new regression formula tailored to first deciduous molars from a pre-industrial population enhances our ability to extract valuable information concerning odontogenic trajectories. This proves particularly useful in cases where enamel microstructure might be compromised or not clearly visible [8]. Consequently, it facilitates a more accurate reconstruction of early life developmental histories, and potentially enhances accurate age-at-death estimations for infant individuals.

Furthermore, this work expands the existing body of research on growth rates in posterior deciduous teeth, complementing previous research focused on anterior and permanent dentition [54, 55]. Prior studies on first deciduous molars have reported differing developmental patterns both across and within populations and historical periods [35, 54, 55]. These variations are also evident when comparing our findings with those derived from British Medieval populations [51, 53]. Consequently, this emphasizes the need to broaden research to encompass diverse populations from various regions and historical periods. Such an approach is instrumental in acquiring a comprehensive understanding of odontogenic variability, and it aids in establishing geographical and historical standards able to enhance the accuracy of anthropological and archaeological investigations reliant on dental developmental patterns, highlighting the importance of further investigation to attain more accurate and reliable data for deciduous teeth.

In conclusion, employing a multi-analytical approach integrating histological analysis with sex determination through peptide assessment, suggests a potential expansion of histological analysis in archaeological deciduous teeth. This highlights the possibility of conducting further sex-driven investigations, particularly concerning the histology of infants in past populations.

## Supporting information

**S1 Fig. Chromatograms of amelogenin isoforms in individuals from Casalmoro.** The presence of both isoforms, AMELX (time ~30 min) and AMELY (time ~20 min), determines sex

as male. Conversely, the presence of the only AMELX isoform assesses the sex as female. From Casalmoro 3 individuals are estimated as male and 5 as female.

(TIF)

**S2 Fig. Chromatograms of amelogenin isoforms in individuals from Guidizzolo.** The presence of both isoforms, AMELX (time ~30 min) and AMELY (time ~20 min), determines sex as male. Conversely, the presence of the only AMELX isoform assesses the sex as female. From Guidizzolo were identified 5 females and 12 males.

(TIF)

**S3 Fig. Linear models to estimate the crown formation time from prism lengths on first deciduous upper and lower molars.** The regression formula for upper molars is  $Y = 0.315 X$  and the estimated mean DSR was  $3.17 \mu\text{mday}^{-1}$ . The regression formula for lower molars is  $Y = 0.318 X$  and the estimated mean DSR was  $3.15 \mu\text{mday}^{-1}$ .

(TIF)

**S4 Fig. Plots of enamel extension rate during the lifetime of each individual.** The plots show changes in EER during the lifetime of each individual. Black lines represent the moment of ALs appearance, which are associated with stress events.

(PDF)

**S1 Table. Crown initiation and crown completion times in first deciduous molars reported in the literature.** Ci times are reported in days after fertilization (considering a gestation length of 39 weeks), whereas Cc times are reported in days after birth.

(XLSX)

## Acknowledgments

We acknowledge the *Soprintendenza Archeologica, Belle Arti e Paesaggio per le Province di Cremona, Lodi e Mantova* for granting us the permission to conduct the analysis. The authors thank the *Fondazione Cassa di Risparmio di Modena* for funding the nLC-MS system at the *Centro Interdipartimentale Grandi Strumenti* of UNIMORE. Dr. Diego Pinetti and Dr. Filippo Genovese are thanked for the assistance during LC-MS analyses.

## Author Contributions

**Conceptualization:** Luca Bondioli, Alessia Nava, Stefano Benazzi.

**Data curation:** Stefano Magri, Owen Alexander Higgins, Federico Lugli, Sara Silvestrini, Antonino Vazzana.

**Formal analysis:** Stefano Magri, Luca Bondioli.

**Funding acquisition:** Stefano Benazzi.

**Investigation:** Stefano Magri, Owen Alexander Higgins, Federico Lugli, Sara Silvestrini, Luca Bondioli.

**Project administration:** Stefano Benazzi.

**Resources:** Antonino Vazzana, Stefano Benazzi.

**Software:** Stefano Magri, Luca Bondioli.

**Supervision:** Alessia Nava, Stefano Benazzi.

**Validation:** Owen Alexander Higgins, Federico Lugli, Sara Silvestrini, Luca Bondioli.

**Visualization:** Stefano Magri, Luca Bondioli.

**Writing – original draft:** Stefano Magri.

**Writing – review & editing:** Stefano Magri, Owen Alexander Higgins, Federico Lugli, Sara Silvestrini, Antonino Vazzana, Luca Bondioli, Alessia Nava, Stefano Benazzi.

## References

1. Hillson S. Dental Anthropology. Dental Anthropology. 2nd ed. Cambridge: Cambridge University Press; 2023. <https://doi.org/10.1017/9781108381550>
2. Guatelli-Steinberg D. What teeth reveal about human evolution. What Teeth Reveal about Human Evolution. Cambridge University Press; 2016. <https://doi.org/10.1017/CBO9781139979597>
3. Boyde A. Estimation of age at death of young human skeletal remains from incremental lines in the dental enamel. Third international meeting in forensic immunology, medicine, pathology and toxicology. Wiley-Liss; 1963. 36–37.
4. Bromage TG, Dean MC. Re-evaluation of the age at death of immature fossil hominids. *Nature* 1985; 317: 525–527. <https://doi.org/10.1038/317525a0> PMID: 19093314
5. Nava A, Coppa A, Coppola D, Mancini L, Dreossi Di, Zanini F, et al. Virtual histological assessment of the prenatal life history and age at death of the Upper Paleolithic fetus from Ostuni (Italy). *Sci Rep* 2017; 7: 9427. <https://doi.org/10.1038/s41598-017-09773-2> PMID: 28842603
6. Smith TM, Reid DJ, Sirianni JE. The accuracy of histological assessments of dental development and age at death. *J Anat*. 2006; 208: 125–138. <https://doi.org/10.1111/j.1469-7580.2006.00500.x> PMID: 16420385
7. Müller W, Nava A, Evans D, Rossi PF, Alt KW, Bondioli L. Enamel mineralization and compositional time-resolution in human teeth evaluated via histologically-defined LA-ICPMS profiles. *Geochim Cosmochim Acta*. 2019; 255: 105–126. <https://doi.org/10.1016/j.gca.2019.03.005>
8. Nava A, Bondioli L, Coppa A, Dean C, Rossi PF, Zanolli C. New regression formula to estimate the prenatal crown formation time of human deciduous central incisors derived from a Roman Imperial sample (Velia, Salerno, Italy, I-II cent. CE). *PLoS One*. 2017; 12: 0180104. <https://doi.org/10.1371/journal.pone.0180104> PMID: 28700601
9. Nava A, Frayer DW, Bondioli L. Longitudinal analysis of the microscopic dental enamel defects of children in the Imperial Roman community of Portus Romae (necropolis of Isola Sacra, 2nd to 4th century CE, Italy). *J Archaeol Sci Rep*. 2019; 23: 406–415. <https://doi.org/10.1016/j.jasrep.2018.11.007>
10. Peripoli B, Gigante M, Mahoney P, McFarlane G, Coppa A, Lugli F, et al. Exploring prenatal and neonatal life history through dental histology in infants from the Phoenician necropolis of Motya (7th–6th century BCE). *J Archaeol Sci Rep*. 2023; 49: 104024. <https://doi.org/10.1016/j.jasrep.2023.104024>
11. Joannes-Boyau R, Adams JW, Austin C, Arora M, Moffat I, Herries AIR, et al. Elemental signatures of Australopithecus africanus teeth reveal seasonal dietary stress. *Nature* 2019; 572: 112–115. <https://doi.org/10.1038/s41586-019-1370-5> PMID: 31308534
12. Kubat J, Nava A, Bondioli L, Bourgon N, Demeter F, Peripoli B, et al. Dietary strategies of Pleistocene Pongo sp. and Homo erectus on Java (Indonesia). *Nat Ecol Evol*. 2023; 7: 279–289. <https://doi.org/10.1038/s41559-022-01947-0> PMID: 36646949
13. Li Q, Nava A, Reynard LM, Thirlwall M, Bondioli L, Müller W. Spatially-Resolved Ca Isotopic and Trace Element Variations in Human Deciduous Teeth Record Diet and Physiological Change. *Environmental Archaeology*. 2020; 13: 1–11. <https://doi.org/10.1080/14614103.2020.1758988>
14. Nava A, Fiorin E, Zupancich A, Carra M, Ottoni C, Di Carlo G, et al. Multipronged dental analyses reveal dietary differences in last foragers and first farmers at Grotta Continenza, central Italy (15,500–7000 BP). *Sci Rep*. 2021; 11: 4261. <https://doi.org/10.1038/s41598-021-82401-2> PMID: 33608594
15. Richards MP, Mays S, Fuller BT. Stable carbon and nitrogen isotope values of bone and teeth reflect weaning age at the Medieval Wharram Percy site, Yorkshire, UK. *Am J Phys Anthropol*. 2002; 119: 205–10. <https://doi.org/10.1002/ajpa.10124> PMID: 12365032
16. Bondioli L, Nava A, Rossi PF, Sperduti A. Diet and health in Central-Southern Italy during the Roman Imperial time. *Acta IMEKO*. 2016; 5: 19–25. [https://doi.org/10.21014/acta\\_imeko.v5i2.333](https://doi.org/10.21014/acta_imeko.v5i2.333)
17. FitzGerald C, Saunders S, Bondioli L, Macchiarelli R. Health of infants in an imperial Roman skeletal sample: Perspective from dental microstructure. *Am J Phys Anthropol*. 2006; 130: 179–189. <https://doi.org/10.1002/ajpa.20275> PMID: 16365859
18. Kierdorf H, Witzel C, Bocaage E, Richter T, Kierdorf U. Assessment of physiological disturbances during pre- and early postnatal development based on microscopic analysis of human deciduous teeth

- from the Late Epipaleolithic site of Shubayqa 1 (Jordan). *Am J Phys Anthropol.* 2021; 174: 20–34. <https://doi.org/10.1002/ajpa.24156> PMID: 33017861
19. Retzius A. Mikroskopiska undersökningar öfver Tändernes, särdeles Tandbenets, struktur. Stockholm: P.A: Norstedt & Söner, 1837.
  20. Wilson DF, Shroff FR. The nature of the striae of Retzius as seen with the optical microscope. *Aust Dent J.* 1970; 15: 162–171. <https://doi.org/10.1111/j.1834-7819.1970.tb03366.x> PMID: 4194293
  21. Antoine D, Hillson S, Dean MC. The developmental clock of dental enamel: A test for the periodicity of prism cross-striations in modern humans and an evaluation of the most likely sources of error in histological studies of this kind. *J Anat.* 2009; 214: 45–55. <https://doi.org/10.1111/j.1469-7580.2008.01010.x> PMID: 19166472
  22. Enamel Boyde A. In: *Teeth. Handbook of Microscopic Anatomy*, vol 5/6. Springer, Berlin, Heidelberg. 1989; 309–473. [https://doi.org/10.1007/978-3-642-83496-7\\_6](https://doi.org/10.1007/978-3-642-83496-7_6)
  23. Dean M. Growth layers and incremental markings in hard tissues; a review of the literature and some preliminary observations about enamel structure in *Paranthropus boisei*. *Journal of Human Evolution.* 1987; 16: 157–172. [https://doi.org/10.1016/0047-2484\(87\)90074-1](https://doi.org/10.1016/0047-2484(87)90074-1)
  24. Lacruz RS, Hacia JG, Bromage TG, Boyde A, Lei Y, Xu Y, et al. The circadian clock modulates enamel development. *J Biol Rhythms.* 2012; 27: 237–245. <https://doi.org/10.1177/0748730412442830> PMID: 22653892
  25. Smith TM. Experimental determination of the periodicity of incremental features in enamel. *J Anat.* 2006; 208: 99–113. <https://doi.org/10.1111/j.1469-7580.2006.00499.x> PMID: 16420383
  26. Neumann AM, Schmidt CX, Brockmann RM, Oster H. Circadian regulation of endocrine systems. *Auton Neurosci.* 2019; 216: 1–8. <https://doi.org/10.1016/j.autneu.2018.10.001> PMID: 30598120
  27. Tao J, Zhai Y, Park H, Han J, Dong J, Xie M, et al. Circadian Rhythm Regulates Development of Enamel in Mouse Mandibular First Molar. *PLoS One.* 2016; 11. <https://doi.org/10.1371/journal.pone.0159946> PMID: 27494172
  28. Zheng L, Ehardt L, McAlpin B, About I, Kim D, Papagerakis S, et al. The tick tock of odontogenesis. *Exp Cell Res.* 2014; 325: 83–89. <https://doi.org/10.1016/j.yexcr.2014.02.007> PMID: 24582863
  29. Zheng L, Seon YJ, Mourão MA, Schnell S, Kim D, Harada H, et al. Circadian rhythms regulate amelogenesis. *Bone.* 2013; 55: 158–165. <https://doi.org/10.1016/j.bone.2013.02.011> PMID: 23486183
  30. Appenzeller O, Gunga HC, Qualls C, Furlan R, Porta A, Lucas SG, et al. A hypothesis: autonomic rhythms are reflected in growth lines of teeth in humans and extinct archosaurs. *Auton Neurosci.* 2005; 117: 115–119. <https://doi.org/10.1016/j.autneu.2004.10.003> PMID: 15664564
  31. Bromage TG, Idaghdour Y, Lacruz RS, Crenshaw TD, Ovsy O, Rotter B, et al. Correction: The swine plasma metabolome chronicles “many days” biological timing and functions linked to growth. *PLoS One.* 2024; 19: e0301870. <https://doi.org/10.1371/journal.pone.0301870> PMID: 38564617
  32. Bromage TG, Juwayeyi YM, Smolyar I, Hu B, Gomez S, Chisi J. Enamel-calibrated lamellar bone reveals long period growth rate variability in humans. *Cells Tissues Organs.* 2011; 194: 124–130. <https://doi.org/10.1159/000324216> PMID: 21525718
  33. Mahoney P, Miszkiewicz JJ, Chapple S, Le Luyer M, Schlecht SH, Stewart TJ, et al. The biorhythm of human skeletal growth. *J Anat.* 2018; 232: 26–38. <https://doi.org/10.1111/joa.12709> PMID: 29023695
  34. Schwartz GT, Reid DJ, Dean C. Developmental aspects of sexual dimorphism in hominoid canines. *Int J Primatol.* 2001; 22: 837–860. <https://doi.org/10.1023/A:1012073601808>
  35. McFarlane G, Guatelli-Steinberg D, Loch C, White S, Bayle P, Floyd B, et al. An inconstant biorhythm: The changing pace of Retzius periodicity in human permanent teeth. *Am J Phys Anthropol.* 2020; 175: 172–186. <https://doi.org/10.1002/ajpa.24206> PMID: 33368148
  36. Reid DJ, Ferrell RJ. The relationship between number of striae of Retzius and their periodicity in imbricational enamel formation. *J Hum Evol.* 2006; 50: 195–202. <https://doi.org/10.1016/j.jhevol.2005.09.002> PMID: 16263151
  37. Canturk N, Atsu SS, Aka PS, Dagalp R. Neonatal line on fetus and infant teeth: An indicator of live birth and mode of delivery. *Early Hum Dev.* 2014; 90: 393–397. <https://doi.org/10.1016/j.earlhumdev.2014.05.002> PMID: 24951074
  38. Dean MC, Spiers KM, Garvoet J, Le Cabec A. Synchrotron X-ray fluorescence mapping of Ca, Sr and Zn at the neonatal line in human deciduous teeth reflects changing perinatal physiology. *Arch Oral Biol.* 2019; 104: 90–102. <https://doi.org/10.1016/j.archoralbio.2019.05.024> PMID: 31176148
  39. Hassett BR, Dean MC, Ring S, Atkinson C, Ness AR, Humphrey L. Effects of maternal, gestational, and perinatal variables on neonatal line width observed in a modern UK birth cohort. *Am J Phys Anthropol.* 2020; 172: 314–332. <https://doi.org/10.1002/ajpa.24042> PMID: 32155296

40. Humanen J, Visnapuu V, Sillanpää M, Löyttyneemi E, Rautava J. Deciduous neonatal line: Width is associated with duration of delivery. *Forensic Sci Int*. 2017; 271: 87–91. <https://doi.org/10.1016/j.forsciint.2016.12.016> PMID: 28073052
41. Janardhanan M, Umadethan B, Biniraj K, Vinod Kumar R, Rakesh S. Neonatal line as a linear evidence of live birth: Estimation of postnatal survival of a new born from primary tooth germs. *J Forensic Dent Sci*. 2011; 3: 8–13. <https://doi.org/10.4103/0975-1475.85284> PMID: 22022132
42. Sabel N, Johansson C, Kühnisch J, Robertson A, Steiniger F, Norén JG, et al. Neonatal lines in the enamel of primary teeth—A morphological and scanning electron microscopic investigation. *Arch Oral Biol*. 2008; 53: 954–963. <https://doi.org/10.1016/j.archoralbio.2008.05.003> PMID: 18589400
43. Sipovac M, Petrovic B, Amzirkov M, Stefanovic S. Enamel incremental markings in the deciduous teeth of children from the Early Bronze and modern ages. *Arch Oral Biol*. 2023; 148: 105635. <https://doi.org/10.1016/j.archoralbio.2023.105635> PMID: 36764086
44. Skinner M, Dupras T. Variation in birth timing and location of the neonatal line in human enamel. In: *J Forensic Sci*. 1993; 38: 1383–1390. <https://doi.org/10.1520/JFS13542J> PMID: 8263481
45. Zanolli C, Bondioli L, Manni F, Rossi P, Macchiarelli R. Gestation Length, Mode of Delivery and Neonatal Line Thickness Variation. *Hum Biol*. 2011; 83: 695–713. <https://doi.org/10.3378/027.083.0603> PMID: 22276969
46. Dirks W, Humphrey LT, Dean MC, Jeffries TE. The relationship of accentuated lines in enamel to weaning stress in juvenile baboons (*Papio hamadryas anubis*). *Folia Primatologica*. 2010; 81: 207–223. <https://doi.org/10.1159/000321707> PMID: 21124031
47. Kurek M, Borowska B, Lubowiedzka-Gontarek B, Rosset I, Żądzińska E. Disturbances in primary dental enamel in Polish autistic children. *Sci Rep*. 2020; 10: 12751. <https://doi.org/10.1038/s41598-020-69642-3> PMID: 32728144
48. Rose JC, Armelagos GJ, Lallo JW. Histological enamel indicator of childhood stress in prehistoric skeletal samples. *Am J Phys Anthropol*. 1978; 49: 511–516. <https://doi.org/10.1002/ajpa.1330490411> PMID: 367176
49. Vacková S, Králík M, Marečková K, Ráčková L, Quade L, Sedláčková L, et al. Human “barcode”: Link between phosphate intensity changes in human enamel and light microscopy record of accentuated lines. *Microchemical Journal*. 2021; 168: 106370. <https://doi.org/10.1016/j.microc.2021.106370>
50. Macchiarelli R, Bondioli L, Debénath A, Mazurier A, Tournepiche JF, Birch W, et al. How Neanderthal molar teeth grew. *Nature*. 2006; 444: 748–751. <https://doi.org/10.1038/nature05314> PMID: 17122777
51. Mahoney P. Human deciduous mandibular molar incremental enamel development. *Am J Phys Anthropol*. 2011; 144: 204–214. <https://doi.org/10.1002/ajpa.21386> PMID: 20740658
52. Mahoney P. Incremental enamel development in modern human deciduous anterior teeth. *Am J Phys Anthropol*. 2012; 147: 637–651. <https://doi.org/10.1002/ajpa.22029> PMID: 22331636
53. Birch W, Dean MC. Corrigendum to “A method of calculating human deciduous crown formation times and of estimating the chronological ages of stressful events occurring during deciduous enamel formation”. *J Forensic Leg Med*. 2014; 22: 127–144. <https://doi.org/10.1016/j.jflm.2013.12.002> PMID: 24485438
54. Aris C, Mahoney P, Deter C. Enamel growth rates of anterior teeth in males and females from modern and ancient British populations. *Am J Phys Anthropol*. 2020; 173: 236–249. <https://doi.org/10.1002/ajpa.24068> PMID: 32369194
55. Aris C. Enamel growth rate variation of inner, mid, and outer enamel regions between select permanent tooth types across five temporally distinct British samples. *Arch Oral Biol*. 2022; 137: 105394. <https://doi.org/10.1016/j.archoralbio.2022.105394> PMID: 35279434
56. Fitzgerald C, Hillson S. Deciduous Tooth Growth in an Ancient Greek Infant Cemetery. *Front Oral Biol*. 2009; 13: 178–183. <https://doi.org/10.1159/000242414> PMID: 19828993
57. McFarlane G, Loch C, Guatelli-Steinberg D, Bayle P, Le Luyer M, Sabel N, et al. Enamel daily secretion rates of deciduous molars from a global sample of children. *Arch Oral Biol*. 2021; 132: 105290. <https://doi.org/10.1016/j.archoralbio.2021.105290> PMID: 34695672
58. Dean MC, Humphrey L, Groom A, Hassett B, Dean C. Variation in the timing of enamel formation in modern human deciduous canines. *Arch Oral Biol*. 2020; 147: 104719. <https://doi.org/10.1016/j.archoralbio.2020.104719> PMID: 32361553
59. Guatelli-Steinberg D, Floyd BA, Dean MC, Reid DJ. Enamel extension rate patterns in modern human teeth: Two approaches designed to establish an integrated comparative context for fossil primates. *J Hum Evol*. 2012; 63: 475–486. <https://doi.org/10.1016/j.jhevol.2012.05.006> PMID: 22748383
60. Shellis RP. Variations in growth of the enamel crown in human teeth and a possible relationship between growth and enamel structure. *Arch Oral Biol*. 1984; 29: 697–705. [https://doi.org/10.1016/0003-9969\(84\)90175-4](https://doi.org/10.1016/0003-9969(84)90175-4) PMID: 6594102

61. Bromage TG, Lacruz RS, Hogg R, Goldman HM, McFarlin SC, Warshaw J, et al. Lamellar bone is an incremental tissue reconciling enamel rhythms, body size, and organismal life history. *Calcif Tissue Int*. 2009; 84: 388–404. <https://doi.org/10.1007/s00223-009-9221-2> PMID: 19234658
62. Mahoney P, McFarlane G, Pitfield R, O'Hara MC, Miszkiewicz JJ, Deter C, et al. A structural biorhythm related to human sexual dimorphism. *J Struct Biol*. 2020;211. <https://doi.org/10.1016/j.jsb.2020.107550> PMID: 32553779
63. AlQahtani SJ, Hector MP, Liversidge HM. Brief communication: The London atlas of human tooth development and eruption. *Am J Phys Anthropol*. 2010; 142: 481–490. <https://doi.org/10.1002/ajpa.21258> PMID: 20310064
64. Mahoney P. Dental fast track: Prenatal enamel growth, incisor eruption, and weaning in human infants. *Am J Phys Anthropol*. 2015; 156: 407–421. <https://doi.org/10.1002/ajpa.22666> PMID: 25388809
65. Cappellini E, Welker F, Pandolfi L, Ramos-Madrugal J, Samodova D, Rütther PL et al. Early Pleistocene enamel proteome from Dmanisi resolves *Stephanorhinus* phylogeny. *Nature*. 2019; 574: 103–107. <https://doi.org/10.1038/s41586-019-1555-y> PMID: 31511700
66. Parker GJ, Yip JM, Eerkens JW, Salemi M, Durbin-Johnson B, Kiesow C, et al. Sex estimation using sexually dimorphic amelogenin protein fragments in human enamel. *J Archaeol Sci*. 2019; 101: 169–180. <https://doi.org/10.1016/j.jas.2018.08.011>
67. Lugli F, Figus C, Silvestrini S, Costa V, Bortolini E, Conti S, et al. Sex-related morbidity and mortality in non-adult individuals from the Early Medieval site of Valdarò (Italy): the contribution of dental enamel peptide analysis. *J Archaeol Sci Rep*. 2020; 34: 102625. <https://doi.org/10.1016/j.jasrep.2020.102625>
68. Lugli F, Di Rocco G, Vazzana A, Genovese F, Pinetti D, Cilli E, et al. Enamel peptides reveal the sex of the Late Antique 'Lovers of Modena.' *Sci Rep*. 2019; 9: 13130. <https://doi.org/10.1038/s41598-019-49562-7> PMID: 31511583
69. Bansal AK, Shetty DC, Bindal R, Pathak A. Amelogenin: A novel protein with diverse applications in genetic and molecular profiling. *Journal of Oral and Maxillofacial Pathology*. 2012; 16: 395–399. <https://doi.org/10.4103/0973-029X.102495> PMID: 23248473
70. Birch W, Dean C. Rates of enamel formation in human deciduous teeth. *Front Oral Biol*. 2009; 13: 116–120. <https://doi.org/10.1159/000242402> PMID: 19828981
71. Dean MC, Humphrey L, Groom A, Hassett B. Variation in the timing of enamel formation in modern human deciduous canines. *Arch Oral Biol*. 2020; 114: 104719. <https://doi.org/10.1016/j.archoralbio.2020.104719> PMID: 32361553
72. FitzGerald CM, Saunders SR. Test of histological methods of determining chronology of accentuated striae in deciduous teeth. *Am J Phys Anthropol*. 2005; 127: 277–290. <https://doi.org/10.1002/ajpa.10442> PMID: 15584065
73. Šešelj M. Brief communication: An analysis of dental development in Pleistocene Homo using skeletal growth and chronological age. *Am J Phys Anthropol*. 2017; 163: 531–541. <https://doi.org/10.1002/ajpa.23228> PMID: 28432824
74. Witzel C. Echoes from birth—Mutual benefits for physical and forensic anthropology by applying increment counts in enamel of deciduous teeth for aging. *Anthropologischer Anzeiger*. 2014; 71: 87–103. <https://doi.org/10.1127/0003-5548/2014/0386> PMID: 24818441
75. Ballarini A. *Storia E Archeologia Del Territorio Mantovano Tra VII E XI Secolo: Studio di una realtà territoriale e nuove prospettive di ricerca*. Edizioni Accademiche Italiane; 2014.
76. Menotti EM. Elementi per la conoscenza del Mantovano nell'Alto Medioevo: le necropoli di via San Martino di Guidizzolo e di San Faustino a Casalmoro. *Annali Benacensi Atti Del XIV Convegno Archeologico Benacense*. 1999: 91–117.
77. Giovannini F. *Natalità, Mortalità e Demografia dell'Italia Medievale sulla Base dei Dati Archeologici* BAR Publishing. 2001. <https://doi.org/10.30861/9781841711775>
78. Bierbrauer V. *Aspetti archeologici di Goti, Alamanni e Longobardi*. In: Pugliese Carratelli G. *Magistra Barbaritas. I barbari in Italia*. Milano. Ed. Scheiwiller-Credito Italiano; 1984.
79. Manicardi A. *San Lorenzo di Quingentole: Archeologia, Storia ed Antropologia*. Mantova: SAP Società Archeologica s.r.l.; 2001.
80. Molnar S. Human Tooth Wear, Tooth Function and Cultural Variability. *Am J Phys Anthropol*. 1971; 34: 175–189. <https://doi.org/10.1002/ajpa.1330340204> PMID: 5572602
81. Granja R, Araújo AC, Lugli F, Silvestrini S, Silva AM, Gonçalves D. Unbalanced sex-ratio in the Neolithic individuals from the Escoural Cave (Montemor-o-Novo, Portugal) revealed by peptide analysis. *Sci Rep*. 2023; 13: 19902. <https://doi.org/10.1038/s41598-023-47037-4> PMID: 37964077
82. Stewart NA, Gerlach RF, Gowland RL, Gron KJ, Montgomery J. Sex determination of human remains from peptides in tooth enamel. *Proc Natl Acad Sci U S A*. 2017; 114: 13649–13654. <https://doi.org/10.1073/pnas.1714926115> PMID: 29229823

83. Lugli F, Cipriani A, Capecchi G, Ricci S, Boschin F, Boscato P, et al. Strontium and stable isotope evidence of human mobility strategies across the Last Glacial Maximum in southern Italy. *Nat Ecol Evol*. 2019; 3: 905–911. <https://doi.org/10.1038/s41559-019-0900-8> PMID: 31086279
84. Schindelin J, Arganda-Carreras I, Frise E, Kaynig V, Longair M, Pietzsch T, et al. Fiji: An open-source platform for biological-image analysis. *Nature Methods*. 2012; 676–682. <https://doi.org/10.1038/nmeth.2019> PMID: 22743772
85. Koller M, Stahel WA. Sharpening Wald-type inference in robust regression for small samples. *Comput Stat Data Anal*. 2011; 55: 2504–2515. <https://doi.org/10.1016/j.csda.2011.02.014>
86. Wood SN. *Generalized Additive Models: an introduction with R* 2ed. CRC Press; 2006.
87. Maechler M, Rousseeuw P, Croux C, Todorov V, Ruckstuhl A, Salibián-Barrera M, et al. *robustbase: Basic Robust Statistics*. 2023. Available: <http://robustbase.r-forge.r-project.org/>
88. Rholff FJ. *tpsDig, digitize landmarks and outlines, version 2.05*. Department of Ecology and Evolution, State University of New York at Stony Brook. 2006.
89. R Core Team. *R: A Language and Environment for Statistical Computing*. Vienna, Austria: R Foundation for Statistical Computing; 2023.
90. Wood SN. Fast stable restricted maximum likelihood and marginal likelihood estimation of semiparametric generalized linear models. *J R Stat Soc Series B Stat Methodol*. 2011; 73: 3–36. <https://doi.org/10.1111/J.1467-9868.2010.00749.X>
91. Holst KK, Budtz-Jørgensen E. Linear latent variable models: the lava-package. *Comput Stat*. 2013; 28: 1385–1452. <https://doi.org/10.1007/S00180-012-0344-Y>
92. Lunt RC, Law DB. A review of the chronology of calcification of deciduous teeth. *J Am Dent Assoc*. 1974; 89: 599–606. <https://doi.org/10.14219/jada.archive.1974.0446> PMID: 4606136
93. Hillson S. *Dental Anthropology*. University College London, editor. Cambridge University Press; 1996. <https://doi.org/10.1017/CBO9781139170697>
94. Lunt RC, Law DB. A review of the chronology of eruption of deciduous teeth. *J Am Dent Assoc*. 1974; 89: 872–879. <https://doi.org/10.14219/jada.archive.1974.0484> PMID: 4609369
95. Mahoney P. Intraspecific variation in M1 enamel development in modern humans: implications for human evolution. *J Hum Evol*. 2008; 55: 131–147. <https://doi.org/10.1016/j.jhevol.2008.02.004> PMID: 18439653
96. Garn SM, Burdi AR. Prenatal ordering and postnatal sequence in dental development. *J Dent Res*. 1971; 50: 1407–1414. <https://doi.org/10.1177/00220345710500060701> PMID: 5289048
97. Burdi AR, Garn SM, Miller RL. Developmental Advancement of the Male Dentition in the First Trimester. 1970; 49: 889. <https://doi.org/10.1177/00220345700490043201> PMID: 5269391
98. Cunningham C, Scheuer L, Black S. *Developmental Juvenile Osteology*. 2 ed. London: Academic Press, 2016.